Single bubble sonoluminescence: Investigations of the emitted pressure wave with a fiber optic probe hydrophone

Z. Q. Wang, R. Pecha, B. Gompf, and W. Eisenmenger
1. Physikalisches Institut, Universität Stuttgart, Pfaffenwaldring 57, D-70550 Stuttgart, Germany
(Received 27 July 1998)

In single bubble sonoluminescence (SBSL) in addition to the short light pulses, the bubble emits in the collapse phase a pressure wave that can be measured with a fiber optic probe hydrophone with high spatial resolution (100 μm) and a rise time of 5 ns. In a systematic study we have characterized the width and the amplitude of the emitted pressure wave in dependence of the driving pressure, the gas concentration, and the water temperature. The width of the emitted acoustic wave increases with increasing gas concentration and increasing driving pressure from about 7 ns to more than 30 ns in the stability range, where SBSL can be observed. In contrast to the emitted light intensity, the water temperature has only little influence on the emitted acoustic wave. Theoretical considerations using the Gilmore equation show good agreement with the experimental data. [S1063-651X(99)08002-2]

PACS number(s): 78.60.Mq, 43.25.+y

I. INTRODUCTION

Cavitation always occurs when the pressure in a liquid drops below a critical value, the cavitation threshold, either due to an acoustic field or due to high streaming velocities. Normally, a large number of cavitation bubbles grow and collapse in this case with a broad distribution of bubble radii. This transient cavitation leads to the so-called ''cavitation noise,'' the superposition of the pressure waves emitted by a large number of bubbles [1]. Due to the statistical behavior of this phenomenon it is difficult to analyze the physical mechanisms behind it. On the other hand, the radiated pressure wave surrounding a collapsing bubble is an important aspect in the studies of cavitation damage, cavitation-related sonochemical effects, and the ultrasonic medical imaging with microbubbles as contrast agent. Many experimental studies have been concentrated on the cavitation noise in a small bandwidth region below 1 MHz [2,3]. The measurement of the emitted pressure wave of single sonoluminescing bubbles, though their behavior may be different from that of transient cavitation bubbles, will be very helpful for the understanding of the dynamics and the effects of these bubbles, and to verify the theoretical studies on the radiated acoustic waves of collapsing bubbles.

In 1990 Gaitan *et al.* [4] demonstrated that a single gas bubble can be trapped in water in the pressure antinode of a standing sound field of about 20 kHz, emitting a short light pulse each cycle. In addition to the light, these small single bubbles also emit a pressure wave. But opposite to transient cavitation bubbles, these single bubbles are well defined and highly reproducible, which make them a model system for investigations of the fundamental physical mechanisms involved in energy concentration, cavitation damage, and sonochemistry. Cordry was the first who reported on the acoustic pulse emitted in single bubble sonoluminescence (SBSL) [5], but his results were limited by the bandwidth of the hydrophone and he gave no values for the amplitude and the width of the emitted acoustic pulse. Matula *et al.* [6], using a piezoelectric hydrophone with a larger bandwidth (100 MHz), claimed that the rise time of the acoustic pulse is about 5 ns and that the amplitude is about 1.7 bar at 1 mm above the bubble at a driving pressure of 1.5 bars. They also show that the pressure wave is emitted at the minimum bubble radius and they were able to detect the pulses emitted from the rebounds.

In this paper we present the systematic study of the pressure waves emitted from single bubbles as a function of the parameters influencing also the emitted light intensity, namely, driving pressure, gas concentration, and water temperature. For the investigations we used a fiber optic probe hydrophone (FOPH) developed in our institute [7]. Besides its high temporal and spatial resolution, this kind of hydrophone has the advantage compared to piezoelectric hydrophones that it is an absolute ultrasonic wide-band reference standard with an accuracy of about 5%. The experimental setup is described in Sec. II. The dependence of the width and amplitude of the acoustic wave on the gas concentration, driving pressure, and temperature will be presented in Sec. III, followed by a discussion about the mechanism of the acoustic emission and the role of nonlinear absorption in the formation of the 7–30-ns-wide acoustic pulses.

II. EXPERIMENTAL SETUP

The principle of the FOPH was described in an earlier paper [7]. The tip of a 100/140-μm glass fiber, which guides a 812 nm laser light, acts as the acoustic sensing element (Fig. 1). The optical reflectance at the fiber end-face is linked to the pressure amplitude via the index of refraction-density relationship. When the pressure increases, the density, and hence the refractive indices of the liquid and the fiber are increased. However, due to the low compressibility of the solid fiber material the change of the index of refraction of the liquid prevails. The resulting change of the optical reflectance is registered with a photodiode and corresponds to the time-dependent pressure amplitude.

The impulse response of the FOPH was determined by a shock wave excitation method [8]. The shock wave was generated by a self-focusing electromagnetic generator designed

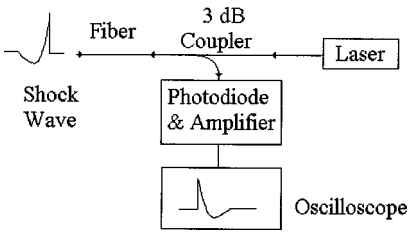

FIG. 1. Experimental configuration of the fiber optic probe hydrophone (FOPH). A pressure pulse changes the refractive index of water and thereby the reflectance at the fiber/water interface. This change is detected by a photodiode and reflects the time-dependent pressure amplitude.

for extracorporeal lithotripsy. The response of the FOPH to the acoustic field of about 30 MPa at the geometric focus of the shock wave generator excited at 19 kV was recorded and averaged over 10 acquisitions. This response exhibits an overshoot within about 80 ns after the rising edge and a smooth decay thereafter. The overshoot is due to the nearly rigid reflection of the acoustic wave at the fiber end-face and the diffracted waves from the edges of the fiber tip [7] and can be described by the diffraction of the acoustic wave by the fiber end-face [8]. By approximating the response of the FOPH to the shock wave excitation as a time step function (except in the overshoot region), we were able to construct the impulse response of the FOPH and to evaluate the shock wave generated by the self-focusing electromagnetic generator. The shock front obtained by the deconvolution of the measured signal with the impulse response of the FOPH is represented in Fig. 2. A rise time of about 5 ns has been obtained. The true shock front rise time is on the order of 1 ns as the shock wave thickness in water is about 1 μm [9]. Nevertheless, a rise time of 5 ns is enough for the characterization of commercial lithotripters and provides us with an ideal tool to measure the acoustic pulse in SBSL at millimeter distance from the bubble, which is still difficult to be resolved by other types of hydrophones.

The air bubble was trapped in a 250-ml spherical quartz glass flask, which was driven at its resonant frequency of about 20 kHz with two piezoelectric disks. For the experiments, we used degassed demineralized water. The gas concentration was controlled with an oximeter. The emitted acoustic wave was detected by the fiber optic probe hydrophone at a distance of about 2.5 mm from the bubble. At that distance, the geometric broadening due to the strong curvature of the wave front and the finite size of the fiber is about

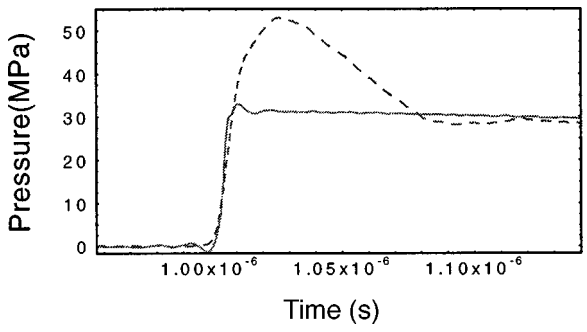

FIG. 2. Response of the FOPH to a pressure step; ----, measured; ——, after deconvolution.

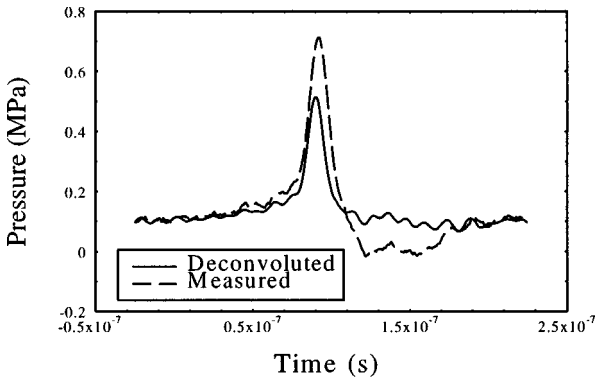

FIG. 3. Typical wave form of the FOPH output measured at 2.5 mm from the collapsing bubble and the corresponding deconvoluted signal.

1.3 ns. The small size of the hydrophone needed for this kind of experiment has, on the other hand, the disadvantage of a low signal-to-noise ratio. But this disadvantage is not specific for the FOPH, because the sensitivity per area is nearly the same for the FOPH and PVDF membrane and needle hydrophones [10]. To increase the signal-to-noise ratio, the output signal of the FOPH was recorded with a Tektronix TD744A sampling oscilloscope and averaged over 100–1000 periods. As trigger signal for the oscilloscope, the filtered output of a much larger and, therefore, more sensitive PVDF hydrophone, placed at about 5 mm from the bubble, was used. The achieved trigger accuracy was about 2 ns. All results shown are deconvoluted with the instrument response function of the hydrophone as described above. A typical wave form recorded with the FOPH together with its deconvolution is shown in Fig. 3.

III. RESULTS

Figure 4 shows the dependence of the full width at half maximum (FWHM) of the emitted pressure wave on the gas concentration. The FWHM at a driving pressure of 1.45 bar and a temperature of 12 °C increases from about 11 ns at an O_2 concentration of 1 mg/l to nearly 25 ns at 2.8 mg/l. In Fig. 5(a) the dependence of the FWHM on the driving pressure at fixed gas concentration is shown. At an O_2 concentration of 2.5 mg/l, the FWHM increases from less than 10 ns at the onset of the sonoluminescence (SL) to about 17 ns at the upper SL threshold. The amplitude of the emitted acoustic wave at 2.5 mm above the bubble also increases with in-

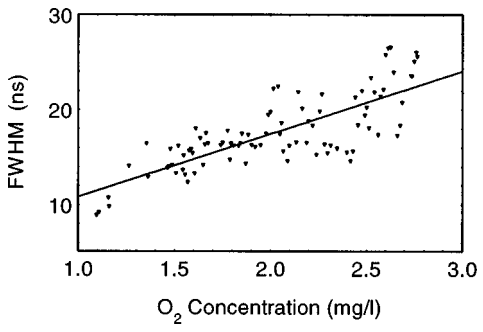

FIG. 4. FWHM of the emitted acoustic wave as a function of gas concentration.

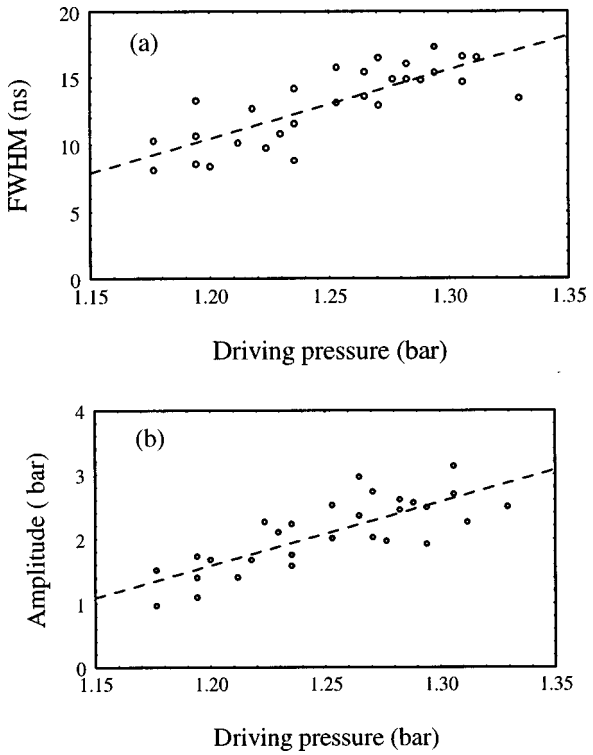

FIG. 5. (a) FWHM and (b) amplitude of the emitted acoustic wave as a function of driving pressure.

creasing driving pressure from about 1 to 3 bars as can be seen from Fig. 5(b). These results agree with the values found by Matula *et al.* for the widths and amplitudes of the emitted sound waves [6]. From this value the initial amplitude of the shock wave at minimum bubble radius is estimated to be about 5000–15 000 bars if only a spherical spreading by $1/r$ is supposed, which underestimates the amplitude of the acoustic wave by neglecting nonlinear effects, as will be discussed in the next section. The relatively large standard deviations in our measurements are mainly the result of space instabilities of the bubble.

In a next step we calculated the frequency components of the acoustic pulses by Fourier transform. As an example, the average spectra of three pulses with about 10 ns widths are given together with the system response function and the attenuation curve for 2.5-mm water in Fig. 6. The comparison with the system response function shows that in the bandwidth limit of our system, the acoustic pulses at this distance can be fully resolved. The comparison with the attenuation curve shows that linear absorption in water can be neglected at 2.5 mm for frequencies below 70 MHz, the bandwidth of our system, which agrees with the theoretical estimations of Matula *et al.* [6].

In SBSL the light intensity increases by a factor of 10 if the water temperature is decreased from 20 to 4 °C. In contrast, we found that the widths and the amplitude of the emitted pressure wave are nearly independent of water temperature. The widths of the pressure wave measured at 3 and 22 °C are shown in Fig. 7. This independence is a remarkable result. The increase of the light and acoustic emission with increasing driving pressure can easily be explained by the bubble dynamics. The different behavior of the two quantities at lower temperatures may be due to the different sensitivity to small changes in the bubble dynamics.

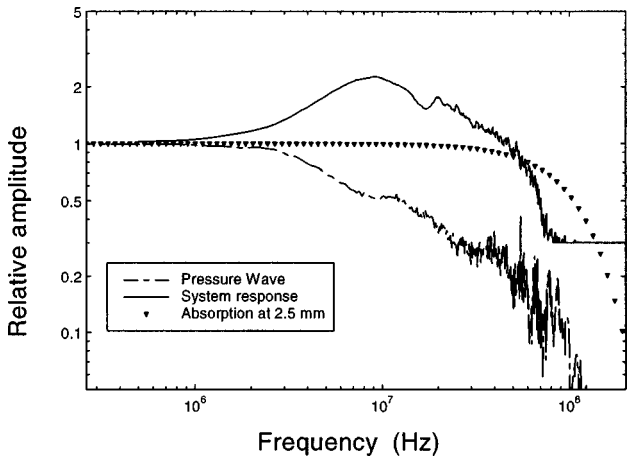

FIG. 6. Frequency analysis of the measured pressure wave (dashed line), the system response (solid line), and the absorption curve for 2.5-mm water (▼).

IV. DISCUSSION

The outgoing pressure wave of a collapsing bubble is related to the gas pressure inside the bubble and to the motion of the bubble wall. Different approximations have been made to describe the bubble dynamics, including the Rayleigh-Plesset equation and Gilmore equation [11]. In this paper, the radiated acoustic pressure in the liquid has been studied using these two equations. With the Rayleigh-Plesset equation for an incompressible fluid, we found that the pulse width of the emitted acoustic wave is about 0.2 ns, in contradiction to our experimental results. If the pulses were so short, we would not have been able to resolve any differences in the pulse width as a function of experimental parameters. In addition, the calculated pulses become narrower at larger driving pressures, which is also in contrast to the measurements.

In a next step the bubble dynamics was described by the Gilmore equation that is derived directly from the enthalpy of the liquid and considers the pressure dependence of the sound velocity. The pressure distribution in the liquid was

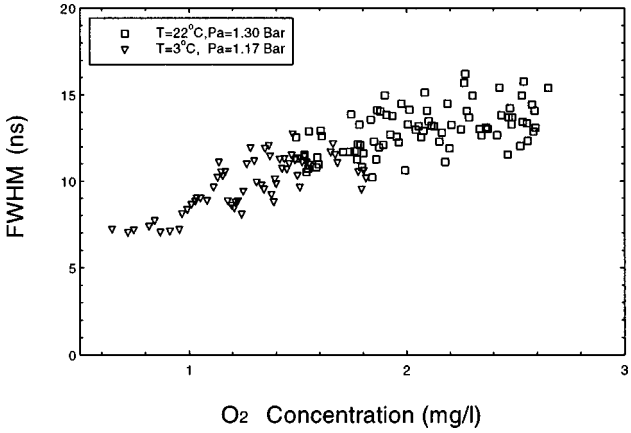

FIG. 7. FWHM of the pressure wave measured at different temperatures and driving pressures, as a function of the gas concentration.

then calculated according to the method proposed by Akulishev [12,13]. This approximation relies on the method of characteristics under the Kirkwood-Bethe approximation. An invariant of the bubble motion G is specified at the bubble surface by $G=R(H+U^2/2)$, where R is the radius of the bubble, H the specific enthalpy of the liquid, and U the bubble wall velocity.

The value of G is unchanged during the propagation along the outgoing characteristic $dr/dt=c+u$, where c is the sound speed in water and u the particle velocity, and can be used to calculate the pressure in the liquid as a function of space and time [13,14]. Due to the finite particle velocity, the distortion of the pressure wave form increases with the distance from the bubble. From some distance, the pressure becomes multivalued, as indicated in the papers of Akulishev. This is physically inadmissible and denotes the discontinuity of the pressure leading to the formation of shock waves. The equal area method was proposed to estimate in this case the pulse width and amplitude [12,13].

Using this method, we found that the emitted acoustic wave at 2.5 mm from a bubble with an equilibrium radius of 6 μm varies from 4 to 15 ns for driving pressures from 1.2 to 1.4 bars. The amplitude of the emitted pressure wave varies from 2 to 10 bars. Both results are in reasonable agreement with our experiments. The variation of the acoustic pulse width and amplitude as a function of gas concentration can be understood by the fact that the equilibrium radius is a function of the gas concentration. Intuitively and as analyzed by Hilgenfeldt and Lohse [15], the equilibrium radii are smaller at smaller gas concentrations. Our calculations show that the width of the emitted pressure waves is 8 ns for a bubble with 4.5-μm equilibrium radius and 12 ns for a bubble of 6-μm radius at a driving pressure of 1.3 bars.

The equations used for calculating the radiated pressure are not strictly valid near the bubble collapse. Other effects should be considered in the model, including thermal conduction and mass diffusion between the gas and the liquid. Also, the gas pressure inside the bubble should not be treated as uniform. On the other hand, our calculations show a reasonable agreement with our experimental data. This agreement leads to an assumption that the formation of a shock wave take place within 30 times the equilibrium radius from the center (about 200 μm). Within this distance, the pulse is broadened by nonlinear effects and the decrease of the amplitude of the pressure wave is faster than the spherical spreading mainly due to energy losses related to the shock formation. This means that the initial pulse width of the pressure wave may be much shorter than the measured and the amplitude of about 15 000 bars is only a lower limit. The energy losses due to the nonlinear propagation of the pressure wave heats the surrounding of the bubble leading to an increased temperature at the bubble surface. This should have an influence on sonochemical reactions, as it has been postulated that some of the reactions take place at the outside of the cavitation bubbles [16].

V. CONCLUSION

The pressure waves emitted in single bubble sonoluminescence have been studied with a fiber optic probe hydrophone. The high spatial and time resolution of the hydrophone allowed us to determine the pulse width and amplitude of the emitted pressure wave as a function of gas concentration, driving pressure, and temperature. The width of the pressure wave is found to increase with the driving pressure and the gas concentration but is independent of the water temperature. Following a finite amplitude analysis, a good agreement between the experimental data and the calculated values was found.

[1] H. G. Flynn, in *Physical Acoustics*, edited by W. P. Mason (Academic, New York, 1964), Vol. 1B.
[2] E. Esche, Acustica **4**, AB208 (1952).
[3] E. Cramer and W. Lauterborn, Appl. Sci. Res. **38**, 209 (1982).
[4] D. F. Gaitan *et al.*, J. Acoust. Soc. Am. **91**, 3166 (1992).
[5] S. M. Cordry, Ph.D. thesis, University of Mississippi, 1995 (unpublished).
[6] T. J. Matula *et al.*, J. Acoust. Soc. Am. **130**, 1377 (1998).
[7] J. Staudenraus and W. Eisenmenger, Ultrasonics **31**, 267 (1993).
[8] Z. Q. Wang *et al.*, J. Appl. Phys. (to be published).
[9] W. Eisenmenger, Acustica **12**, 185 (1962).
[10] W. Eisenmenger *et al.*, in *Proceedings of the World Congress on Ultrasonics, Yokohama, Japan, 1997*, edited by K. Takag (Pacifico, Yokohama, 1997), pp. 18 and 19.
[11] F. R. Young, *Cavitation* (McGraw-Hill, London, 1989).
[12] V. A. Akulishev, in *High Intensity Ultrasonic Fields*, edited by L. D. Rozenberg (Plenum, New York, 1971).
[13] V. A. Akulishev, Sov. Phys. Acoust. **13**, 281 (1968).
[14] E. Cramer, in *Cavitation and Inhomogeneities in Underwater Acoustics*, edited by W. Lauterborn (Springer-Verlag, Berlin, 1979).
[15] S. Hilgenfeldt and D. Lohse, Phys. Fluids **8**, 2808 (1996).
[16] K. S. Suslick, IEEE Trans. Ultrason. Ferroelectr. Freq. Control **UFFC-33**, 143 (1986).